Validation of prospective whole-body bone marrow dosimetry by SPECT/CT multimodality imaging in ^{131}I-anti-CD20 rituximab radioimmunotherapy of non-Hodgkin's lymphoma

Jan A. Boucek[1], J. Harvey Turner[1, 2]

[1] Department of Nuclear Medicine, Fremantle Hospital, Fremantle, WA, Australia
[2] School of Medicine and Pharmacology, University of Western Australia, Australia

Received: 6 July 2004 / Accepted: 24 August 2004 / Published online: 20 November 2004

Abstract. *Purpose:* Radioimmunotherapy (RIT) for relapsed non-Hodgkin's lymphoma is emerging as a promising treatment strategy. Myelosuppression is the dose-limiting toxicity and may be particularly problematic in patients heavily pretreated with chemotherapy. Reliable dosimetry is likely to minimise toxicity and improve treatment efficacy, and the aim of this study was to elucidate the complex problems of dosimetry of RIT by using an integrated SPECT/CT system.
Methods: As a part of a clinical trial of ^{131}I-anti-CD20 rituximab RIT of non-Hodgkin's lymphoma, we employed a patient-specific prospective dosimetry method utilising the whole-body effective half-life of antibody and the patient's ideal weight to calculate the administered activity for RIT corresponding to a prescribed radiation absorbed dose of 0.75 Gy to the whole body. A novel technique of quantitation of bone marrow uptake with hybrid SPECT/CT imaging was developed to validate this methodology by using post-RIT extended imaging and data collection.
Results: A strong, statistically significant correlation (p=0.001) between whole-body effective half-life of antibody and effective marrow half-life was demonstrated. Furthermore, it was found that bone marrow activity concentration was proportional to administered activity per unit weight, height or body surface area (p<0.001).
Conclusion: The results of this study show the proposed whole-body dosimetry method to be valid and clinically applicable for safe, effective RIT.

Keywords: Non-Hodgkin's lymphoma – Rituximab – Radioimmunotherapy – Dosimetry – SPECT/CT

Jan A. Boucek (✉)
Department of Nuclear Medicine, Fremantle Hospital,
Alma St., Fremantle, 6160, WA, Australia
e-mail: Jan.Boucek@health.wa.gov.au
Tel.: +61-89431-2888, Fax: +61-89431-2889

Eur J Nucl Med Mol Imaging (2005) 32:458–469
DOI 10.1007/s00259-004-1692-9

Introduction

A clinical study of ^{131}I-rituximab anti-CD20 chimeric monoclonal antibody (MabThera, Roche, Australia) radioimmunotherapy (RIT) of relapsed/refractory non-Hodgkin's lymphoma (NHL) commenced at Fremantle Hospital in 1999. Between April 1999 and March 2002, 42 courses of RIT were administered to 38 patients in a pilot study that evolved into an Australian phase II multicentre clinical trial [1]. Comparable clinical results of RIT of NHL have been reported elsewhere [1–5], and it appears that this promising treatment modality may be used increasingly for relapsed NHL.

Myelosuppression is the dose-limiting side-effect of RIT. Prospective individualised bone marrow dosimetry may minimise the risk of myelotoxicity, especially in patients whose marrow reserve is compromised by tumour infiltration and prior therapy. However, published dosimetry methods in RIT have not adequately addressed the issue of bone marrow self-irradiation, since the main limitation of current dosimetric methods is the absence of reliable methodology to measure bone marrow uptake [4, 5]. A more reliable, non-invasive method of estimating absorbed bone marrow dose is required, such as patient-specific prospective dosimetry methodology for RIT, which is based upon assessment of the surrogate total body dose [2, 3]. It has been found experimentally that a mean prescribed dose of 0.75 Gy to whole body, when applied to ^{131}I-anti-CD20 RIT of NHL, causes only modest and self-limited myelotoxicity [1–3]. Our study was designed to validate the dosimetric methodology for prospective estimation of a safe effective mean prescribed dose as a preferred alternative to the conventional oncology paradigm of maximum tolerated dose

[1]. Normograms have been formulated to establish maximum effective mass of whole body as weight in kilograms as a function of gender and height [2, 3]. The maximum effective mass may then be compared with the actual weight of the patient, and the lesser designated as the ideal weight, which may then be used to establish an injected activity. The whole-body dose can be used as a surrogate for absorbed dose to red marrow, provided that two assumptions are valid: that the same ^{131}I injected activity per kilogram of ideal weight would result in a similar activity concentration in the red marrow, and that the whole-body and bone marrow residence times are equivalent. To achieve the same or similar absorbed dose to active marrow, the injected activity per unit of body weight, height or body surface area (BSA) has to be scaled according to whole-body residence time.

We have applied SPECT/CT imaging on a hybrid system to validate a modification of Kaminski's methodology [2, 3] using post-RIT quantitative SPECT imaging, with X-ray-based attenuation correction. Our study utilised the attributes of an integrated SPECT/CT system to contribute to an understanding of the complex problems of dosimetry of RIT with particular relevance to minimising marrow toxicity whilst preserving tumour treatment efficacy.

Materials and methods

Dosimetry methodology – theoretical considerations

Dosimetry of bone marrow, whilst critical, is very difficult to measure in the clinical practice of RIT. The marrow is widely distributed in small pockets inside bone tissue and is not easy to delineate. Furthermore, active bone marrow is not distributed evenly, which compromises estimation of the true radiation absorbed dose fraction estimates. Published dosimetry methods in RIT have not adequately addressed the issue of marrow contribution to bone marrow dose, often being limited to empirical observations. They have not explained fully the observed RIT myelotoxicity [2, 3], although it has been proposed that radiation absorbed doses in the order of 2 Gy to bone marrow will induce myelotoxicity [6, 7].

Internal radiation sources contributing to the overall radiation absorbed dose to bone marrow in RIT can be divided into three compartments: blood, marrow and remainder of body [8, 9]. Using medical internal radiation dose (MIRD) methodology, these three contributing components of active marrow dose may be considered separately. For measured activity due to blood and marrow, a factor is used where haemopoietically active marrow is both target and source ($S_{RM \rightarrow RM}$). In our study, it was assumed that all radioactive sources from blood and marrow compartments are located in active marrow rather than in the whole marrow space, which impacts upon established *S* factors [10–13]. Briefly, initial estimation of active marrow *S* factors as defined in the MIRDOSE3 program [10] makes the implicit assumption that $S_{RM \rightarrow RM} = CF \cdot S_{TM \rightarrow TM}$, where TM represents total marrow and CF expresses the cellularity fraction of active red marrow (RM). However, this approximation may greatly underestimate the absorbed fraction, particularly at low electron energies where the absorbed fraction should approach unity in the case of red marrow. We used the approach of Bolch et al. [12] to compute energy-dependent absorbed fractions. For ^{131}I, we calculated the non-penetrating absorbed fraction in spine (where the expected cellularity fraction was 0.7) to be 0.66 and therefore $S_{RM \rightarrow RM,el}$ to be $1.73 \cdot 10^{-5}$ mGy/MBq·s. However, to compute the contribution from photons of ^{131}I to active marrow self-dose, $S_{RM \rightarrow RM,phot}$, we used an approach similar to that of Stabin et al. [10]. We computed the photon absorbed fraction ($\varphi_{marrowVOI \rightarrow marrowVOI,phot}$) by using Monte Carlo modelling of a Cristy-Eckerman phantom of spine for photon emissions of ^{131}I, then multiplied the photon absorbed fraction by the cellularity fraction (0.7 for spine). The *S* factor used in this study was thus $S_{RM \rightarrow RM,phot} = 5.68 \cdot 10^{-6}$ mGy/MBq·s. Therefore, absorbed dose considerations are region-related to spine rather than to whole marrow, and the appropriate *S* factor was thus $S_{RM \rightarrow RM} = 2.3 \cdot 10^{-5}$ mGy/MBq·s.

Absorbed radiation doses to active marrow from penetrating radiation from the remainder of the body are due to either circulation of radioactivity in body fluids or accumulation in organs such as spleen, liver and kidney. It may be assumed that no activity is accumulated in the actual bone of the skeleton. Current practice employs MIRD methodology and associated *S* factors. The *S* factor for ^{131}I and remainder of body (RB), which includes neither active marrow itself nor trabecular and cortical bone tissues, is $S_{RB \rightarrow RM} = 4.38 \cdot 10^{-7}$ mGy/MBq·s and was derived from the published methods of Coffey and Watson [14].

Extended imaging and data collection protocol

All 27 patients in our extended ^{131}I-rituximab RIT dosimetric study underwent a standard treatment protocol as described previously [1]. Briefly, humanised chimeric rituximab was radiolabelled in-house by the chloramine-T method. An initial tracer activity of 200 MBq ^{131}I-rituximab was injected intravenously. Subsequently, whole-body gamma camera imaging at 1 h and 4 and 7 days was used to determine the effective half-life of the radioiodinated antibody. The therapy activity was then computed using our modification of the total body dosimetry quantitation approach proposed by Wahl [2, 3] which takes into account lean body weight and whole-body clearance rate.

All patients had relapsed NHL after one to five prior courses of chemotherapy and often immunotherapy, and 44% had bone marrow infiltration demonstrated on single-site trephine biopsy. Estimation of the extent of tumour involvement of bone marrow was not performed, given the known sampling error, and our patients are not deemed ineligible for treatment on the basis of an arbitrary 25% bone marrow tumour involvement which precluded therapy with ^{90}Y-Zevalin in reported studies [15].

We performed blood sampling at the same time as the tracer whole-body imaging was performed, that is day 0, day 4 or 5 and day 7 in 17 patients. The activity concentration of ^{131}I in plasma was measured using a gamma counter, Wizard 1480 (Wallac, Finland). All 27 patients on the extended dosimetric protocol had SPECT/CT scans performed 5–7 days after administration of the therapy dose. Additional lumbar spine static imaging (5-min anterior and posterior views) was performed during tracer scanning. A cohort of six typical patients (Table 1) had SPECT/CT post-therapy scans performed at three time points.

Table 1. Characteristics of 27 patients on study of whom six patients (bold) underwent serial post-RIT imaging

Patient no.	Sex	Age	Stage (yrs)	NHL/ WHO 2001	Prior Rx	BM	Response
1	**F**	**77**	**II**	**Small lymphocytic**	**2**	**–**	**CR**
2	M	64	II	Follicular grade 3	3	–	CR
3	M	70	IV	Small lymphocytic	3	+	PD
4	F	58	II	Follicular grade 2	4	–	CR
5	M	52	II	MALT	4	–	CRu
6	**F**	**64**	**III**	**Follicular grade 2/3**	**3**	**–**	**PR**
7	M	35	II	Follicular grade 1	3	–	CR
8	F	58	IV	Mantle cell	1	+	CR
9	F	38	IV	Small lymphocytic	3	+	PD
10	F	76	III	Follicular grade 2	1	–	PR
11	F	52	III	Follicular grade 3	5	–	PD
12	**M**	**54**	**IV**	**Follicular grade 1**	**4**	**+**	**CR**
13	M	81	IV	Follicular grade 2	2	+	PR
14	**F**	**52**	**II**	**Follicular grade 2**	**5**	**–**	**CR**
15	F	60	IV	Follicular grade 1	1	+	CR
16	M	64	II	Follicular grade 1	4	–	CRu
17	M	65	IV	Follicular grade 3	2	+	CR
18	M	78	III	Mantle cell	4	+	PD
19	F	49	IV	Follicular grade 1	2	+	CR
20	M	63	III	Follicular grade 1	4	–	PD
21	M	81	IV	Follicular grade 1	4	+	PR
22	**M**	**57**	**IV**	**Follicular grade 1**	**4**	**–**	**CR**
23	M	54	IV	Follicular grade 3	5	–	CR
24	M	63	IV	Follicular grade 2	1	+	CR
25	F	58	II	Follicular grade 1	4	–	CRu
26	M	65	IV	Small lymphocytic	3	+	PR
27	**M**	**77**	**II**	**MALT**	**4**	**–**	**CR**

M male, *F* female, *MALT* mucosa-associated lymphoid tissue, *CR* complete response, *CRu* unconfirmed complete response, *PD* progressive disease, *PR* partial response

Uptake quantitation using hybrid SPECT/CT scans

All patients were scanned after receiving RIT and calculated uptakes relate to therapy administrations of 1.63–3.45 GBq ^{131}I-rituximab calculated to deliver a fixed total body dose of 0.75 Gy in each patient. The field of view (FOV) of scans was centred on the pelvis or known tumour masses. The pelvic FOV contained a relatively high volume of bone marrow and the three marrow compartments in which uptakes were measured: spinal, pelvic and femoral marrow. The effective axial FOV for GE HawkEye SPECT/CT scans is approximately 39 cm. SPECT was acquired using 90 projections and a 128×128 matrix with varying frame time depending upon count rate. The CT component of acquisition used full-circle rotation, 40 slices with 140 kVp voltage and 2 mA current. Each scan was reconstructed using standard automatic ordered subset expectation maximisation (OSEM) reconstruction as implemented on the nuclear medicine eNTegra workstation. All SPECT images were attenuation corrected by means of integrated CT using CT-based attenuation correction.

Marrow cavities in spine, pelvis and femur were identified on CT. In order to delineate bone marrow on SPECT slices, regions of interest (ROIs) were drawn on CT slices identifying the marrow tissue. Preserving geometry, the marrow ROIs were then transferred onto corresponding SPECT slices of SPECT/CT scan, allowing uptake quantitation (Figs. 1, 2). The marrow ROIs were divided into three volume of interest (VOI) compartments: spinal marrow, pelvic marrow and femoral marrow. Average counts in each marrow VOI were then converted to activity and activity concentration using calibration factors (see Appendix 1 for a detailed description of calibration of the SPECT/CT scanner). Activity concentration in the bone marrow was then estimated based on activity in the marrow VOIs by correcting for yellow marrow and bone tissue volumes. The correcting factor for yellow marrow volume R was based on ICRP 70 marrow cellularity values and the correcting factor q for bone tissue was based on measurement of CT intensities in marrow VOI (see Appendix 2 for a detailed description of the method).

Measuring active marrow uptake allowed assessment of merit of our assumptions in that the same administered activity per kilogram of ideal weight would result in the same or a similar activity concentration in the active marrow at the time of administration when comparing our active marrow measurements with theoretically expected activities. The corrected activity concentration in spinal marrow was plotted as a function of activity administered per unit of weight, activity administered per unit of patient height and activity administered per unit of BSA. The BSA was computed using DuBois' equation BSA=0.007184 $H^{0.725}W^{0.425}$, where BSA is expressed in square metres, H is the patient's height in centimetres and W is the patient's weight in kilograms.

To compare measured and expected bone marrow concentrations, we defined three parameters, which should be uniform for all patients undergoing our administration protocol:

1. Weight-corrected marrow loading L_{wt}:

$$L_{wt} = \frac{A_{RM,conc}W}{A_{in\,i}} \quad (1)$$

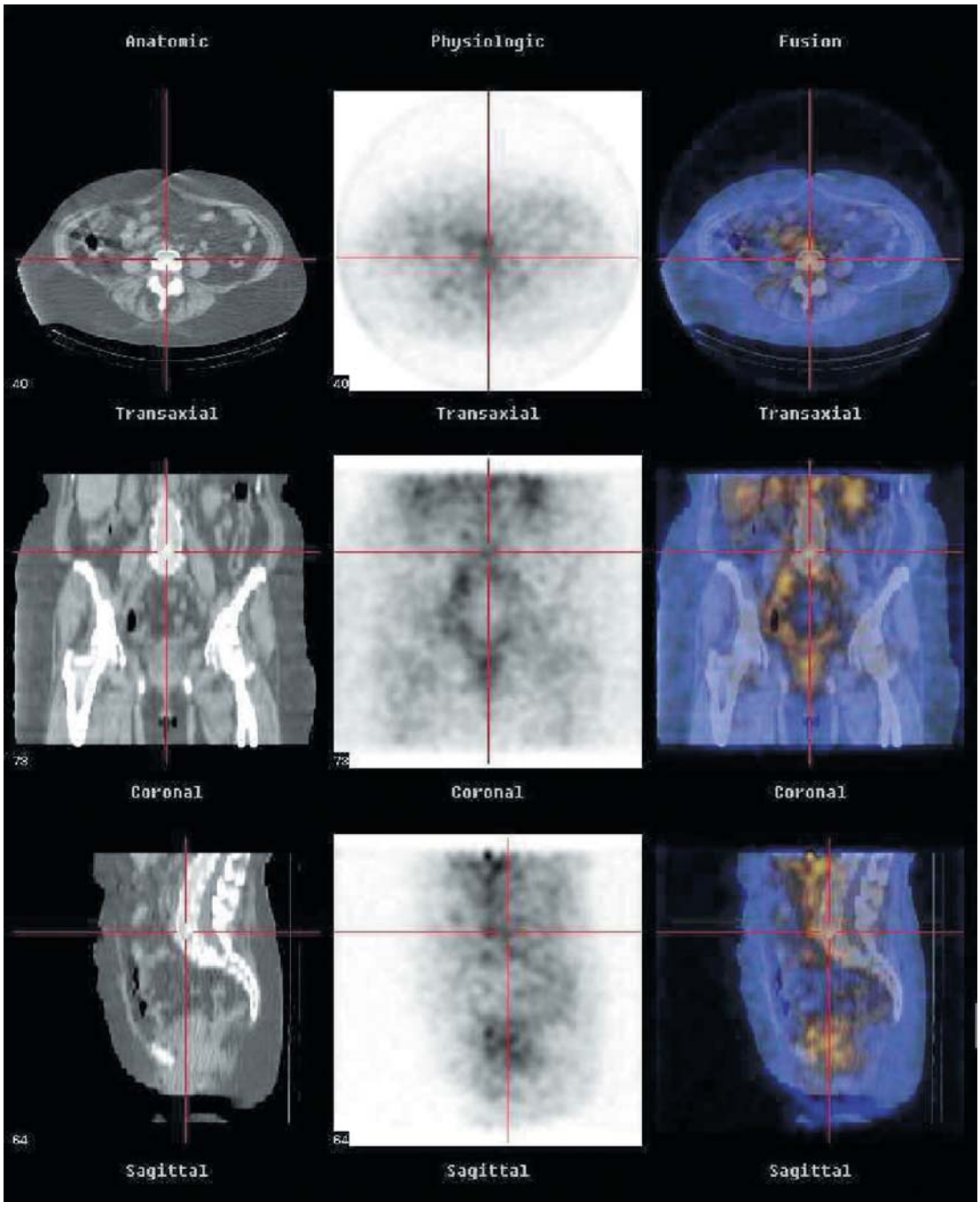

Fig. 1. CT/SPECT multimodality images of ^{131}I-rituximab uptake in the abdomen, pelvis and proximal femur at 5 days after RIT. The *crosshair* indicates focal activity in trabecular marrow of a lumbar vertebra.

2. Height-corrected marrow loading L_{ht}:

$$L_{ht} = \frac{A_{RM,conc} h}{A_{inj}} \tag{2}$$

3. BSA-corrected marrow loading L_{BSA}:

$$L_{BSA} = \frac{A_{RM,conc} BSA}{A_{inj}} \tag{3}$$

where $A_{\mathrm{RM,conc}}$ is the measured activity concentration in red marrow extrapolated to the time of injection, w is the weight of a patient in kilograms, h is the height of a patient in centimetres and A_{inj} is the activity injected in SI units.

Bone marrow clearance rate measurements by SPECT/CT imaging

In a limited cohort of six patients, three SPECT/CT scans were performed on day 5, day 7 and days 10–12 after their therapy administration. These six patients were logistically available for more intensive study and were representative of the study population of 27 patients whose clinical characteristics are outlined in Table 1. The active marrow activity concentration was measured

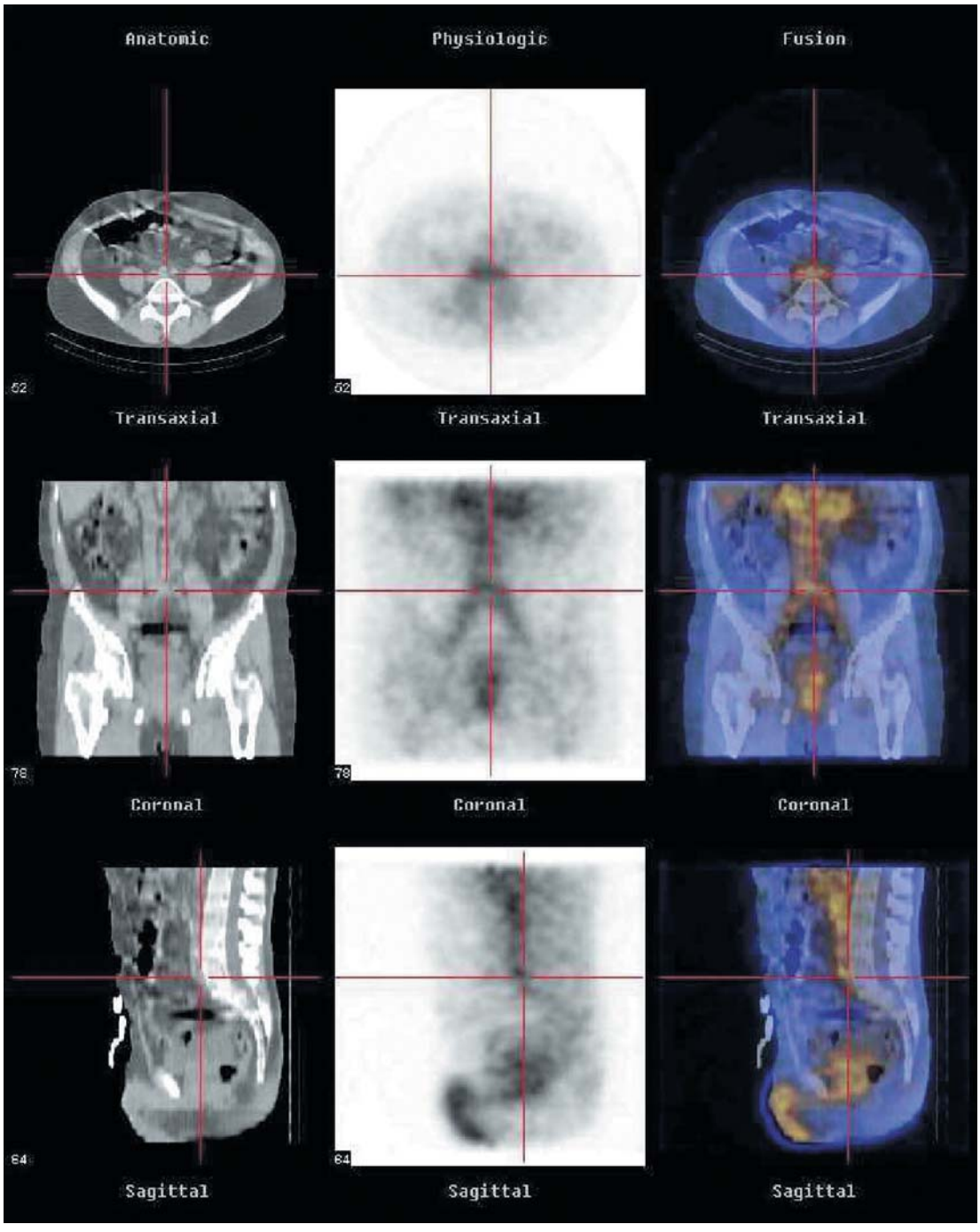

Fig. 2. CT/SPECT multimodality images of ^{131}I-rituximab uptake in the abdomen, pelvis and proximal femur at 5 days after RIT. The *crosshair* indicates focal activity in the aorta vascular space and para-aortic lymph nodes.

in spinal, pelvic and femoral compartments using SPECT/CT imaging for each time point. These concentrations were then plotted as a function of time after administration. The effective half-life of ^{131}I in red marrow was then established by fitting a mono-exponential function.

Measuring active marrow effective half-life of the antibody allowed assessment of merit of our assumption of equivalence of total body and bone marrow effective half-lives. The SPECT/CT-measured active marrow effective half-lives for three compartments, separately, and for three compartments together were compared with whole-body effective half-lives measured by whole-body imaging using the non-parametric Wilcoxon signed ranks test.

Comparison of marrow toxicity and marrow dosimetry

Given the assumption that the whole-body clearance rate is the same as the bone marrow clearance rate, and assuming that the effect of uptake time in bone marrow is negligible, we can estimate

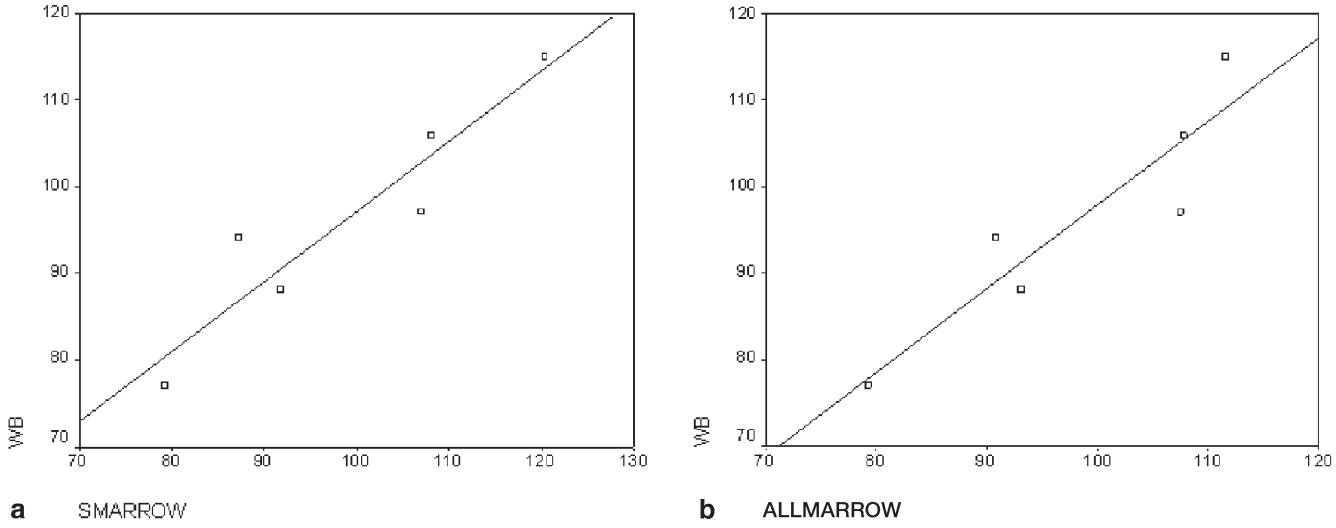

Fig. 3. The effective half-life of ^{131}I-rituximab in whole-body measured by planar imaging plotted against that in the spinal marrow (*SMARROW*, **a**) and in the whole marrow (*ALLMARROW*, **b**) measured by the SPECT/CT method.

Table 2. Values of measured activity concentrations in spinal, pelvic and femoral marrow compartments using SPECT/CT methodology, extrapolated to time of infusion of ^{131}I-rituximab

Compartment	Average (kBq/ml)	Median (kBq/ml)	Minimum (kBq/ml)	Maximum (kBq/ml)	Standard deviation
Spinal (n=27)	84.3	80.2	34.8	172.45	27.8
Pelvic (n=21)	91.2	85.7	44.7	187.2	28.63
Femoral (n=18)	133.3	129.0	74.9	255.5	36.3

absorbed doses to red marrow from marrow internal sources (blood and marrow). Furthermore, using whole-body clearance rates and knowledge of administered activities, we can estimate absorbed radiation doses from activity in whole-body remainder. The sum of self-marrow absorbed dose and remainder of body absorbed dose is the total measured absorbed dose to red marrow. To calculate absorbed dose to active marrow, we measured injected activity, whole-body effective half-life, extrapolated red marrow activity concentration measured on SPECT/CT scans and patient height and weight for correction to BSA.

We compared our measurements of bone marrow uptake (weight-corrected loading, height-corrected loading and BSA-corrected loading) and derived dosimetry quantities (absorbed dose to active marrow, BSA-corrected absorbed dose to active marrow) with myelotoxicity parameters (platelet and neutrophil counts). Myelotoxicity was characterised in terms of decrease in platelet and neutrophil counts defined by the ratio of nadir to pretreatment baselines and the logarithm of such ratios.

To ascertain whether there were any statistically significant linear relationships between myelotoxicity parameters (platelet and neutrophil nadirs) and dosimetry and uptake quantities (weight-corrected loading, height-corrected loading and BSA-corrected loading), linear regression analysis was performed.

Results

Bone marrow clearance rates measured by SPECT/CT imaging

In an intensive study of six typical patients (Table 1), the effective half-life of ^{131}I-rituximab in active marrow was measured using SPECT/CT scans at three time points after RIT. We showed that there was no statistically significant difference between the whole-body half-life and the half-life in any of the marrow compartment and total marrow VOIs. More importantly, there was a statistically significant correlation (Pearson correlation test, r=0.936, p=0.006) and linear relationship (t=5.307, p=0.01) between the whole-body imaging effective half-life and the spinal marrow effective half-life. The same also applied to whole-body imaging effective half-life and the total marrow effective half-life correlation (Pearson correlation test, r=0.919, p=0.001) with a linear relationship (t=4.669, p=0.01): $T_{1/2,WB}$=1.335+0.966 $T_{1/2,ALL\_MARROW}$, where effective half-lives are expressed in hours.

Despite the limited size of the sample, a strong relationship between these two sets of measurements is demonstrated in the whole-body versus marrow plots (Fig. 3).

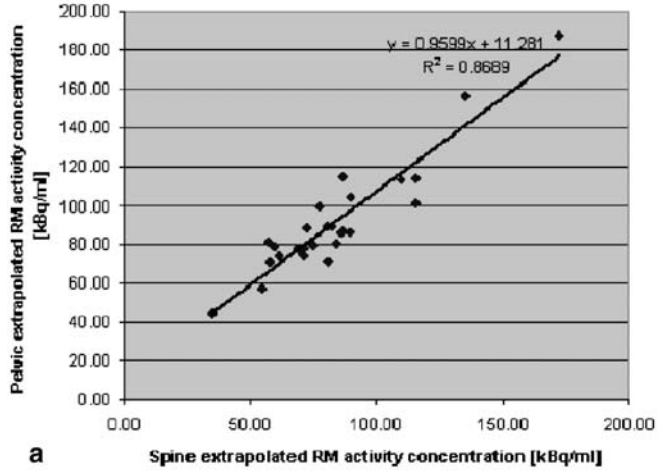

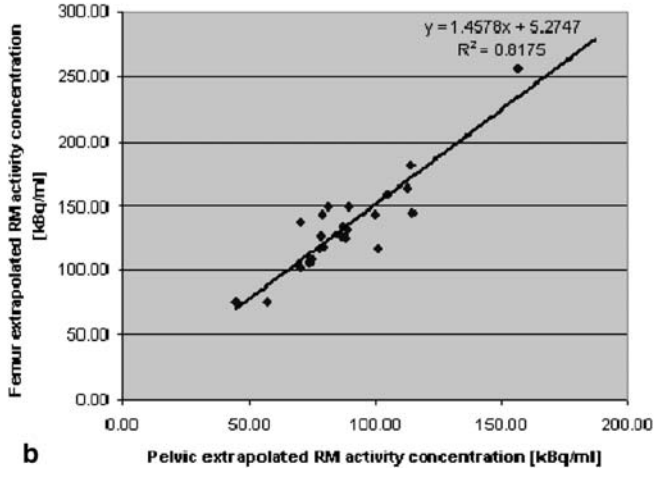

Fig. 4. The activity concentration of ^{131}I-rituximab, extrapolated to the time of administration, in pelvic and spinal marrow (**a**) and pelvic and femoral marrow (**b**) measured by the SPECT/CT method.

Bone marrow uptake measured using SPECT/CT scans

SPECT/CT scans obtained in 27 patients on day 5 after administration of ^{131}I-rituximab therapy doses were used for quantitation of marrow uptake. Active marrow uptake in spinal, pelvic and femoral compartments was quantified and corrected for inactive marrow and bone tissue volume. These values were then extrapolated to the therapy administration time using whole-body effective half-lives measured by whole-body imaging, yielding median activity concentrations for active marrow in spine, pelvis and femur of 80.2, 85.7 and 129 kBq/ml, respectively (Table 2).

Measurements of activity concentration in spine, pelvis and femoral compartments correlated very closely as assessed using the Pearson correlation test (p<0.001, Fig. 4). Furthermore, there was a statistically significant linear relationship (p<0.001, Fig. 5) between extrapolated corrected activity concentration and each of the parameters associated with administered activity (activity

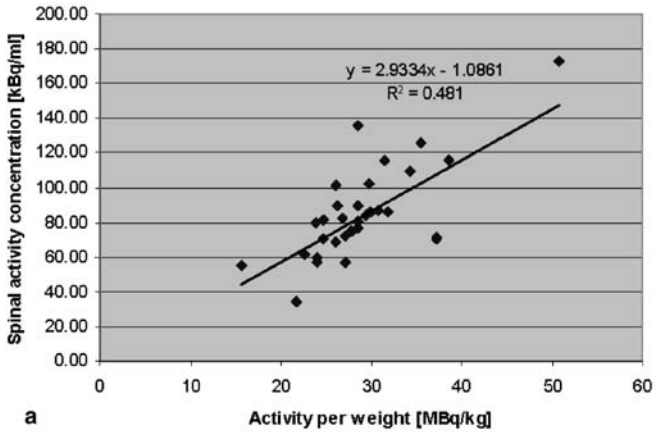

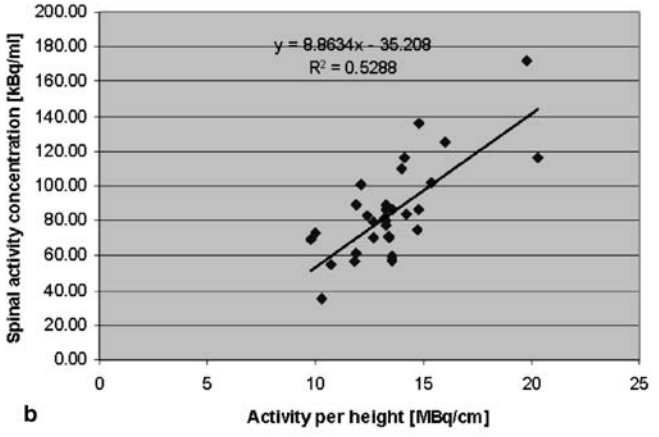

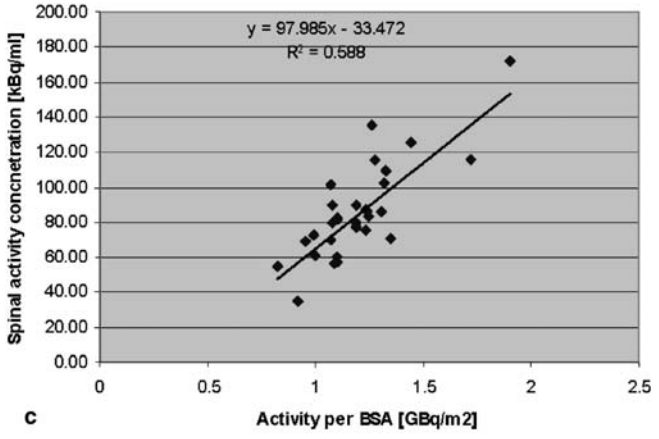

Fig. 5. The activity concentration of ^{131}I-rituximab in spinal red marrow, extrapolated to the time of administration and plotted against administered activity **a** per kilogram of patient weight, **b** per centimetre of patient height and **c** per square metre of BSA.

administered per unit of weight, per unit of height and per unit of BSA). The best correlation and the most significant linear relationship were found between spinal marrow activity concentration and administered activity per metre squared of BSA (r=0.767, t=6.65, p<0.001; Fig. 5c).

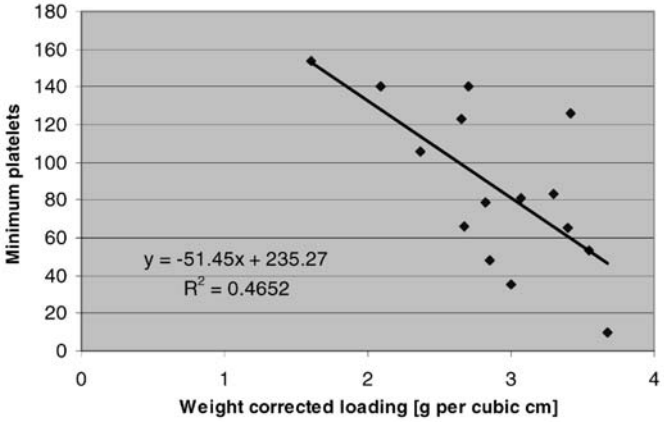

Fig. 6. Platelet nadir as a function of weight-corrected loading following administration of ^{131}I-rituximab RIT.

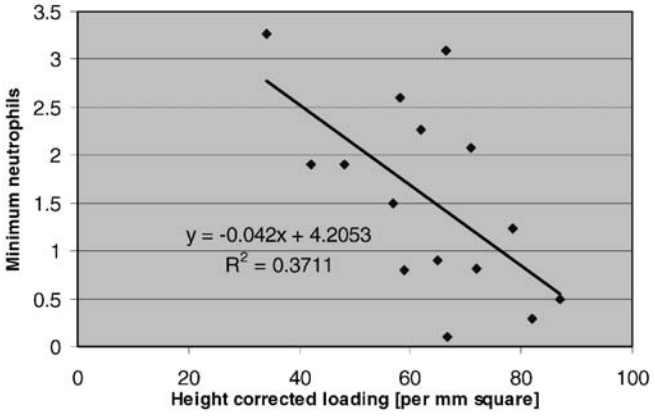

Fig. 7. Neutrophil nadir as a function of height-corrected loading following administration of ^{131}I-rituximab RIT.

Table 3. Results of Pearson test of correlation between myelotoxicity results and measured uptake and dosimetry parameters (significant correlations at the 0.05 level are shown in bold)

	Absorbed dose to active marrow (Gy)	BSA-corrected absorbed dose to active marrow (Gy)	Height-corrected loading	Weight-corrected loading	BSA-corrected loading
Neutrophil nadir	–0.424	**–0.598**	**–0.609**	–0.459	**–0.576**
Platelet nadir	**–0.554**	**–0.551**	**–0.605**	**–0.682**	**–0.664**
Platelet decrease	0.449	**0.643**	**0.580**	0.486	**0.564**
Logarithm of platelet decrease	**–0.542**	**–0.632**	–0.509	–0.481	–0.519
Neutrophil decrease	0.494	**0.654**	0.473	0.444	0.479
Logarithm of neutrophil decrease	**–0.523**	**–0.573**	–0.399	–0.403	–0.420

n=15

Table 4. Results of linear regression testing applied to myelotoxicity results and measured uptake and dosimetry parameters (significant correlation at 0.05 level in bold)

	Platelet nadir	Neutrophil nadir
Weight-corrected loading	**t=–3.363, p=0.005**	*t*=–1.864, *p*=0.085
Height-corrected loading	**t=–2.739, p=0.017**	**t=–2.77, p=0.016**
BSA-corrected loading	**t=–3.205, p =0.007**	**t=–2.537, p=0.025**
Active marrow absorbed dose	**t=–2.401, p=0.032**	*t*=–1.687, *p*=0.115
BSA-corrected active marrow absorbed dose	**t=–2.381, p =0.033**	**t=–2.69, p=0.019**

n=15

Dosimetry results

The median absorbed dose to spinal active marrow in 27 patients was 1.56 Gy (1.09–1.90 Gy) with a standard deviation of 0.20 Gy. The dominant contribution was found to be from active marrow self-dose: median 0.98 Gy (0.55–1.33 Gy) with a standard deviation of 0.18 Gy. Given that we computed the dose using S factors for a standard man [16], correction should be made for different weights and amounts of active marrow by scaling the dose using BSA. The median BSA-corrected absorbed dose in our population was 1.50 Gy (1.14–1.88 Gy) with a standard deviation of 0.19 Gy. The dominant contribution was found to be from BSA-corrected active marrow self-dose: median 0.96 Gy (0.57–1.33 Gy) with a standard deviation of 0.19 Gy.

Comparison of marrow toxicity and marrow dosimetry

There was a statistically significant correlation at the 0.05 level between BSA-corrected active marrow absorbed dose and all myelotoxicity parameters measured (platelet nadir, neutrophil nadir, platelet and neutrophil decreases, logarithms of platelet and neutrophil decreases). Statistically significant correlations were found between platelet nadir and all uptake and dose quantities (weight-corrected loading, height-corrected loading, BSA-corrected loading, absorbed dose to active marrow, BSA-corrected absorbed dose to active marrow). Details of the correlation results obtained using the Pearson correlation test are shown in Table 3.

There was a statistically significant linear relationship between all uptake and dose quantities and platelet

elotoxicity will be minimised. Direct measurement of bone marrow uptake is more accurate but is technically demanding and is unlikely to be practical in routine clinical practice. Therefore whole-body dosimetry offers an acceptable compromise, offering sufficient accuracy and functionality for safe and effective clinical practice of RIT in lymphoma.

Potential problems and limitations in our SPECT/CT method comprise three sources of systematic error: partial volume effect, scatter contribution and specific problems associated with bone marrow uptake quantitation. The influence of the partial volume effect will be less pronounced than in routine SPECT because marrow VOIs are of a considerably greater size. We modelled partial volume effects on quantitation of spinal activity by employing Cristy-Eckerman's phantom and using an intensity ratio of 2:1. The maximum computed error in our estimation was less than 18%, which may be even further reduced by our ROI drawing technique, which leaves some space at the edge of the spinal column. Another problem with quantitation of bone marrow is an expectation that marrow VOIs may be drawn only at the sites of confluence of bone tissues and marrow tissues. This, however, is not always possible. For example, for spine ROIs, the space between vertebrae is included in the spinal marrow VOI, which may lead to underestimation of activity concentration of the order of 10–15%. Furthermore, for quantitation purposes, we assumed that the cellularity fraction (fraction of active marrow in the total marrow space) is equal to average values quoted in ICRP 70 [18]. Each time the radioactivity in marrow VOI is corrected by dividing by the cellularity fraction, we used average values rather than patient-specific values. The cellularity fraction may vary widely, and this was especially true in our patient population, given that each of the patients had undergone prior courses of chemotherapy and often radiotherapy. We obtained very similar red marrow concentrations in pelvic and spinal compartments (median 80.2 kBq/ml for spine and 85.7 kBq/ml for pelvis), but the haematopoietically active concentrations in femoral compartments were much higher after correction for the cellularity fraction. This may be due to different vascularity in the femoral compartment or perhaps the cellularity fraction of 0.25 [18] was inappropriately low for our patient population. A cellularity fraction of 1.5 times higher (0.375, i.e. 37.5%) would have provided a median in the femoral marrow compartment concordant with other compartments (median 86 kBq/ml) in our patients.

Direct measurement of radiation absorbed dose to bone marrow on biopsy samples obtained in patients undergoing ^{131}I-labelled monoclonal antibody RIT for NHL showed that haematological grade III/IV toxicity was manifested in all patients in whom the actual marrow dose exceeded 2 Gy [7]. This elegant but demanding and invasive direct methodology is impractical for routine clinical application. However, these definitive findings accord well with our SPECT/CT imaging results, where no grade IV haematological toxicity was evident. Specifically, in our series, patients received a median 1.56 Gy dose (range 1.09–1.90 Gy) and no patient exceeded the 2 Gy myelotoxicity threshold. Published reports of instances of grade III/IV haematological toxicity occurring in patients adjudged to have received marrow doses of less than 1 Gy after RIT for NHL [4, 15] should be viewed with some degree of scepticism, it being likely that the discordant results may be ascribable to methodological shortcomings. We have successfully correlated red marrow uptake and dosimetric parameters measured by our SPECT/CT technique with myelotoxicity parameters. Pearson correlation coefficients between absorbed doses to red marrow, computed using MIRDOSE *S* factors, and the haematological toxicity were found to be weaker and not statistically significant. For example, a correlation coefficient of R=–0.554 was obtained when using calculated *S* factors while R=–0.475 was obtained when MIRDOSE *S* factors were used. Our calculated *S* factors much better suit the nature of dosimetry of ^{131}I -anti-CD20 antibody. Even though systematic errors are likely to be of the order of 20%, these errors will represent an inherent underestimation. Further conservatism is incorporated in our approach by prescribing a whole-body dose of 0.75 Gy, which, in our patient series, gave rise to a SPECT/CT measured red marrow dose of 1.09–1.90 Gy without significant myelotoxicity.

Conclusion

We have validated a practical prospective individual dosimetry method using whole body as a surrogate organ for the estimation of red marrow dose [1–3] for RIT of NHL. This method is based upon scaling the administered activity using whole-body effective half-life and ideal weight of a patient in the expectation that absorbed dose to bone marrow will be directly proportional to the effective half-life of radiolabelled antibody in the whole body and that it will decrease linearly with the ideal weight of a patient. We measured marrow uptake using a novel technique employing SPECT/CT hybrid imaging and found that whole-body effective half-life and red marrow half-life strongly correlated (p=0.001) and demonstrated a statistically significant linear relationship (t=4.669, p=0.01), showing their equivalence. Furthermore, marrow uptake correlated strongly (p<0.001) with the administered activity per unit of weight, height or BSA, demonstrating a statistically significant relationship between marrow uptake and activity administered per unit of weight, height or BSA. The most significant relationship was that between marrow activity concentration and activity administered and unit of BSA (t=6.65, p<0.001). We conclude that whole body may be safely used as a surrogate organ for haemopoietically active marrow for prospective individualised critical organ do-

nadir, with the most significant relationship (p=0.005) being that with weight-corrected loading (Fig. 6). Furthermore, there was a statistically significant linear relationship between height-corrected loading, BSA-corrected loading and BSA-corrected absorbed dose to active marrow and neutrophil nadir at the 0.05 level of significance, with the most significant relationship (p=0.016) being that with height-corrected loading (Fig. 7). The results of linear regression testing are summarised in Table 4.

Discussion

Bone marrow dosimetry calculation in RIT of lymphoma is difficult. There is uncertainty regarding migration of malignant and normal B cells in and out of bone marrow and, in addition, lymph nodes in proximity to bone marrow may be infiltrated. It is apparent that conventional approaches to marrow dosimetry may not accurately account for doses actually received by the critical organ during radiolabelled antibody therapies [4]. Clinical approaches using whole-body imaging of surrogates such as ^{111}In-ibritumomab tiuxetan for dosimetric biodistribution studies, as mandated by the FDA in the USA for ^{90}Y-Zevalin RIT, have not predicted toxicity in patients [15]. The empirical administered activity of 11 MBq/kg for ^{90}Y-Zevalin RIT for NHL leads to greater myelotoxicity than that reported for ^{131}I-tositumomab (Bexxar) or ^{131}I-rituximab, based on prospective individual patient dosimetry and prescribed as a radiation absorbed dose of 0.75 Gy to total body [17].

There are at least two major areas where conventional dosimetry may be failing to provide accurate answers: quantitation of bone marrow uptake and quantitation of absorbed radiation doses to bone marrow. In this study we have attempted to validate the clinical whole-body dosimetry method by more extensive quantitative imaging and analysis of a cohort of patients undergoing ^{131}I-rituximab RIT of NHL at the prescribed dose of 0.75 Gy to whole body.

If haemopoietically active marrow contains CD20-positive cells, uptake in active marrow will be elevated (Fig. 1). This will lead to a radiation absorbed dose deposited in the active marrow which cannot be accounted for by any method currently used in clinical practice. Macey et al. [9] proposed the use of planar imaging of the lumbar spine for quantification. In our extended protocol, we incorporated lumbar spine planar imaging, although it became apparent that this technique was not reliable in our patients. Our SPECT/CT imaging data showed clearly that the majority of NHL patients have para-aortic node involvement (Fig. 2), in which uptake is quite intense, although it may not be demonstrable on planar images. Furthermore even after 5 days there is relatively high activity in major blood vessels (Fig. 2), especially in the aorta, which will be in the field of interest on planar lumbar spine images. Counts from involved lymph nodes and aortic activity cannot be easily differentiated from counts from marrow (Figs.1, 2). Thus planar imaging techniques are unlikely to be reliable for accurate bone marrow uptake quantitation for ^{131}I-rituximab in NHL patients.

To quantitate bone marrow uptake, we employed a novel method using hybrid semi-quantitative CT/SPECT imaging to provide accurate dosimetric calculations and allow investigation of certain aspects of our dosimetry protocol, which uses the whole body as a surrogate organ for bone marrow. Our method is based on prior empirical observations and dose escalation trials of radioiodinated murine anti-CD20 antibody in NHL [2, 3], although congruence of whole-body dose and red marrow absorbed dose had not been proved. The whole-body dosimetry method is practical, reproducible and reliable despite the fact that it accounts neither for accumulation of activity in bone marrow due to specific targeting of red marrow nor for different residence times in bone marrow and total body. Two assumptions are implicit in the method: firstly that residence times in whole body and bone marrow are equivalent, and secondly that the activity concentration in red marrow at the time of administration is directly proportional to administered activity per unit of ideal weight.

We tested both of these assumptions against our data and measurements of marrow uptake using SPECT/CT scanning in patients receiving ^{131}I-rituximab RIT for relapsed or refractory NHL. A strong statistically significant correlation between whole-body effective half-life and marrow half-life (Pearson correlation test, r=0.919, p=0.001) as well as a statistically significant linear relationship (t=4.669, p=0.01) was demonstrated. Furthermore, we found that the activity concentration in red marrow at the time of administration was directly proportional to the administered activity per unit of weight, height and BSA (r=0.767, t=6.65, p<0.001). Therefore, we conclude that both assumptions have been validated and are correct. Thus the relatively simple total body dosimetry calculation may be appropriately used as a surrogate for haematopoietic marrow dosimetry.

However, we detected some deviations especially from the second assumption of linear relationships between activity per weight, ideal weight or BSA and activity concentration in marrow. Hence total body dosimetry model differences were skewed; that is, a large difference was found due to overestimation of bone marrow concentration (up to 63%) whilst the maximum underestimation was found to be 33% in the worst case. It may be inferred that the whole-body model of absorbed dose will not produce substantial overestimation of absorbed doses but on some occasions underestimation of absorbed doses will be significant. Thus using our whole-body dosimetry protocol, even though the absorbed dose to bone marrow will vary, errors will favour a conservative estimate of administered activity and the risk of my-

simetry to ensure safe, effective ^{131}I-rituximab RIT of NHL. There have been no adverse clinical events in our patients treated using methodology limiting the prescribed radiation absorbed dose to total body to 0.75 Gy.

Acknowledgements. The technical assistance and advice of Christopher Jones and the data evaluation and statistical analysis by Kerryn Butler-Henderson are gratefully acknowledged. This study was supported in part by Fremantle Hospital Nuclear Medicine Research Fund and the loan of an eNTegra workstation from GE Medical Systems. The phase II clinical trial of ^{131}I-rituximab in NHL is a physician-sponsored study and no commercial funding support has been solicited or received.

Appendix 1

Calibration of SPECT/CT scanner

For quantitation of ^{131}I-rituximab uptake a SPECT/CT hybrid scanner (Millennium VG HawkEye, GE Medical Systems, WI, USA) was used [19]. To accurately quantify organ uptake of ^{131}I using SPECT/CT imaging, a calibration factor must first be obtained to convert SPECT image count density (or count rate in the pixel or region) to the ^{131}I tracer activity concentration for patient images, and thus in the organs, by extrapolation and summation.

For calibration, a standard reference phantom (PET/SPECT Performance Phantom 76-823, Nuclear Associates, NY, USA) with a "Linearity/Uniformity Insert" and a "Hot Lesion Insert" was filled with water and 403 MBq of ^{131}I. The solution was mixed thoroughly to ensure uniform distribution of activity. The phantom was then scanned at 15 time points, each time point corresponding to a different activity concentration of ^{131}I. The acquisition was performed using a standard ^{131}I tumour imaging protocol comprising 90 projections (45 projections for each detector), at 50 s for every projection. The SPECT matrix was 128×128 and the pixel size, 3.45 mm. The CT component of acquisition used a full-circle rotation, 40 slices, with 140 kVp voltage and 2 mA current. Each scan was reconstructed using standard automatic iterative OSEM reconstruction on a nuclear medicine workstation (eNTegra v2.016, GE Medical Systems, WI, USA). All SPECT images were attenuation corrected by means of CT-based attenuation correction.

All SPECT and corresponding CT scans were reconstructed in 128 slices and then exported into Interfile image format. The number of counts was quantified in IDL (Research Systems, CO, USA) programming environment using several programs developed in-house. The calibration strategy comprised placing an ROI where counts or count density is not affected by partial volume effects, which may compromise application of calibration factors. The exclusion of partial volume effects in vitro was achieved by placing ROIs, where counting was performed, inside the phantom cylinder and ensuring that pixels near the walls of the phantom were not included by using an automated computer program written in IDL. The program scanned through the dataset on a slice-by-slice basis. First, the centre of mass in a slice was found and then a circle centred on the centre of mass was drawn in that slice to delineate the ROI. The circle had a diameter which was smaller than the physical diameter of the phantom by at least of one full-width at half-maximum, which was approximately 18 mm. The calibration VOI comprised all ROIs in all relevant slices. Such established count densities in VOIs were then plotted for 15 different activity concentrations. The calibration parameters were established by fitting a linear function onto measured data. The statistical errors were assessed using conventional parametric methods on goodness of fit and confidence intervals.

Calibration of linear function for computation of activity (kBq) in a pixel

$$A_{pix} = aC + b \tag{4}$$

where A_{pix} is activity in a pixel in kBq, C is the number of counts in a pixel per second and a and b are calibration parameters. It should be noted that this is independent of pixel size. Calibration parameters as computed were a=8.0789±0.0579 kBq·s and b=0.0045±0.2109 kBq.

The SPECT/CT calibration is performed using a similar technique to that employed for SUV calibration of PET scanners. It is based on an ideal case of infinite source, that is, as if partial volume effect did not exist. Every implementation of such parameters thus may need to estimate a quantitation error. Errors will be dependent upon the volume and geometry of VOI and sources surrounding the VOI.

Appendix 2

Calculation of active marrow uptake

Uptake of ^{131}I-rituximab in the bone marrow was estimated using marrow VOIs. It is reasonable to assume that the VOI drawn on CT consists of a mixture of cortical bone and bone marrow only. We can then represent the fraction of bone in the VOI as p and the fraction of marrow in the VOI as q, while M is the average intensity of the VOI on the CT image expressed in CT numbers. The mean CT number of bone tissue is 3,000 and mean CT numbers for red marrow and yellow marrow are 1,008 and 965, respectively [20, 21]. Thus the mean CT number of a mixture of yellow and red marrow will be dependent upon the ratio of yellow to red marrow. In practice, the bone marrow density and its CT number are dependent upon the fraction of yellow marrow, which will vary depending

upon the location of bone marrow and the age of the patient. We used the values published in ICRP 23 [16] and ICRP 70 [18]. Active marrow volume fraction R is 0.7 (spinal), 0.48 (pelvic) and 0.25 (femoral), and the respective S numbers for spinal, pelvic and femoral marrow compartments are 995, 986 and 976.

Relationship between correction factors p *and* q

$$1 = p + q \quad M = 3000p + Sq \tag{5}$$

Computation of bone tissue correction factor q

Bone tissue fraction can then be expressed.

$$q = \frac{M - 3000}{S - 3000} \tag{6}$$

Formula for correcting activity concentration for bone tissue and yellow marrow volume

The activity concentration in active marrow (A_{RM}) can then be obtained from activity concentration in bone marrow VOI (A_{CT_VOI}) by correcting by factor q for supporting bone tissue volume and by factor R for yellow marrow volume.

$$A_{RM} = \frac{A_{CT\_VOI}}{qR} \tag{7}$$

References

1. Turner JH, Martindale AA, Boucek J, Claringbold PG, Leahy MF. ^{131}I-Anti CD20 radioimmunotherapy of relapsed or refractory non-Hodgkin's lymphoma: a phase II clinical trial of a non-myeloablative dose regimen of chimeric rituximab radiolabeled in a hospital. Cancer Biother Radiopharm 2003;18:513–24.
2. Wahl RL. Iodine-131 anti-B1 antibody therapy in non-Hodgkin's lymphoma: dosimetry and clinical implications. J Nucl Med 1998;39(suppl):1S–9S.
3. Wahl RL, Kroll S, Zasadny KR. Patient-specific whole-body dosimetry: principles and a simplified method for clinical implementation. J Nucl Med 1998;39(suppl):9S–16S.
4. Wiseman GA, Leigh B, Lamonica D, Kornmehl E, Spies SM, Silverman DHS, et al. Radiation dosimetry results for Zevalin radioimmunotherapy of rituximab-refractory non-Hodgkin lymphoma. Cancer 2002;94:1349–57.
5. DeNardo SJ, DeNardo GL, Kukis D, Shen S, Kroger L, DeNardo DA, et al. ^{67}Cu-2IT-BAT-Lym-1 pharmacokinetics, radiation dosimetry, toxicity and tumour regression in patients with lymphoma. J Nucl Med 1999;40:303–10
6. Turner JH, Martindale AA, Sorby P, Hetherington EL, Fleay R, Hoffman R, et al. Samarium-153 EDTMP therapy of disseminated skeletal metastasis. Eur J Nucl Med 1989;15:784–95.
7. Rizzieri DA, Akabani G, Zalutsky M, Coleman RE, Metzler SD, Bowsher JE, et al. Phase 1 trial study of ^{131}I-labeled chimeric 81C6 monoclonal antibody for the treatment of patients with non-Hodgkin lymphoma. Blood 2004;104:642–8.
8. Sgouros G. Bone marrow dosimetry for radioimmunotherapy: theoretical considerations. J Nucl Med 1993;34:689–94.
9. Macey DJ, DeNardo SJ, DeNardo GL, DeNardo DA, Shen S. Estimation of radiation absorbed doses to the red marrow in radioimmunotherapy. Clin Nucl Med 1995;20:117–25.
10. Stabin MG. MIRDOSE: personal computer software for internal dose assessment in nuclear medicine. J Nucl Med 1996; 37:538–46.
11. Bouchet LG, Bolch WE, Howell RW, Rao DV. S values for radionuclides localized within the skeleton. J Nucl Med 2000; 41:189–212.
12. Bolch WE, Patton PW, Rajon DA, Shah AP, Jokisch DW, Inglis BA. Considerations of marrow cellularity in 3-dimensional dosimetric models of the trabecular skeleton. J Nucl Med 2002;43:97–108.
13. Stabin MG, Eckerman KF, Bolch WE, Bouchet LG, Patton PW. Evolution and status of bone and marrow dose models. Cancer Biother Radiopharm 2002;17:427–33.
14. Coffey JL, Watson EE. Calculating dose from remaining body activity: a comparison of two methods. Med Phys 1979; 6:307–8.
15. Wiseman GA, Kornmehl E, Leigh B, Erwin WD, Podoloff DA, Spies S, et al. Radiation dosimetry results and safety correlations from ^{90}Y-ibritumomab tiuxetan radioimmunotherapy for relapsed or refractory non-Hodgkin's lymphoma: combined data from four clinical trials. J Nucl Med 2003;44: 465–74.
16. Snyder WS et al. Report of the task group on reference man. Pergamon Press, ICRP report No.23. Oxford, UK: International Commission on Radiological Protection; 1974.
17. Juweid ME. Radioimmunotherapy of B-cell non-Hodgkin's lymphoma: from clinical trials to clinical practice. J Nucl Med 2002;43:1507–29.
18. ICRP 70, Basic anatomical and physiological data for use in radiological protection: the skeleton. ICRP publication 70. Oxford, UK: International Commission on Radiological Protection; 1995.
19. Patton JA, Delbeke D, Sandler MP. Image fusion using an integrated, dual-head coincidence camera with X-ray tube-based attenuation maps. J Nucl Med 2000;41:1364–68.
20. Knoos T, Nilsson M, Ahlgren L. A method for conversion of Hounsfield number to electron density and prediction of macroscopic pair production cross-sections. Radiother Oncol 1986;5:337–45.
21. Duck FA. Physical properties of tissue: a comprehensive reference book. New York: Academic Press; 1990.